JEE Journal of Ecological Engineering

Journal of Ecological Engineering 2023, 24(2), 131–139
https://doi.org/10.12911/22998993/156664
ISSN 2299–8993, License CC-BY 4.0

Received: 2022.11.01
Accepted: 2022.12.10
Published: 2023.01.01

Wastewater Treatment Using Activated Carbon Produced from Oil Shale

Mohmmad Ahmad Hamdan[1,2*], Esraa Taha Sublaban[3], Jamil Jawdat Al-Asfar[2], Mai Abdullah Banisaid[4]

[1] Renewable Energy Technology Department, Applied Science Private University, Al Arab street, Amman 11931, Jordan

[2] School of Engineering, The University of Jordan, Queen Rania Street, Amman 11942, Jordan

[3] Department of Science and Technology, National University College of Technology, Hamad Awad Al-Huneiti Street, Amman 11592, Jordan

[4] Attarat Um Ghudran, Wasfi Al Tal Street, Amman 11822, Jordan

* Corresponding author's e-mail: mashamdan@yahoo.com

ABSTRACT

In recent years, many researchers have expressed interest in wastewater treatment using activated carbon produced from cheap raw materials. In this work, an activated carbo-aluminosilicate (ACS) – supported zero-valent iron (ZVI) composite was produced from Um AL-Rasa oil shale mine and examined to eliminate Chromium (VI) from contaminated water. Activation of raw oil shale fine particles (< 212 μm) was chemically performed using 95 and 5% wt of H_2SO_4 and HNO_3, respectively, as activating agents. The activated material was further treated with caustic soda, named ACS, and modified with fine zero-valent iron particles < 212 μm), called ZVI/ACS composite. Kaolin was added to the composite with the ratio: (50 % wt. light kaolin: 50 % wt. ACS), named as ZVI/ACS/K. The XRD analysis for both composites confirmed iron dispersion at 45°. Adsorption experiments were carried out using the two adsorbents ZVI/ACS & ZVI/ACS/K under different values of pH, and adsorbent dosage. The results indicated that the reduction of Chromium was maximum under the 3 pH value and 2.0 gm amount of ZVI/ACS/K. Furthermore, it was found the removal rate was enhanced by 17% and 24.7% when ZVI/ACS & ZVI/ACS/K adsorbents were used, respectively, compared to that when only ACS adsorbent was used alone. Finally, the dependency of Chromium removal on its initial concentration by ZVI/ACS/K adsorbent was also investigated at two different temperatures of 27° and 50°. The results indicated a decrease in the removal rate of the Chromium as the concentration increased at 27°; however, the removal rate previously enhanced at 50° at all initial concentrations.

Keywords: activated carbon, wastewater treatment, removing heavy metal from water.

INTRODUCTION

In recent years, Jordan has suffered from limited water resources and may not be able to meet its freshwater demands shortly. Therefore, securing freshwater resources in terms of quality and quantity is becoming more and more important. One of the main sources that cause water contamination with metals (including Chromium, and Copper) is the industry and exploitation of oil shale.

Nowadays, elimination of pollutants from contaminated water by activated carbon is widely used; it is proven to be a successful method for removing toxic metal ions at various concentrations (El Zayat 2009; Ramana et al., 2010; Danious et al., 2015; Shahrokhi-Shahraki et al., 2021).

Yahya et al. (2020) proposed cobalt ferrite-supported activated carbon (CF-AC) for the elimination of Lead and Chromium ions from contaminated water. They concluded that the ecologically friendly alternative adsorbent created from CF-AC can be employed effectively to remove Cr and Pb(II) ions from tannery wastewater. ZVI was found to be excellent at removing pollutants from wastewater, such as toxic metal ions (Ullah et al., 2020., He et al., 2020). Extensive research work was conducted on removing

metals from wastewater using ZVI stabilized on carbon material, (Qu et al., 2017; Zhou et al., 2014; Congbin et al., 2021).

In recent years, Jordan has suffered from limited water resources and may not be able to meet its freshwater demands shortly. Therefore, securing freshwater resources in terms of quality and quantity is becoming more and more important. One of the main sources that cause water contamination with heavy metals is the exploitation of oil shale, which is one of the activities that take place in Jordan. Oil shale utilization technologies include mining, extraction, products, and by-products, etc. which could pose serious risks to the surrounding environment if these issues are not addressed and treated correctly The present research focused on ZVI stabilization on an activated carbon material produced from Jordanian oil shale and examined its ability to remediate hexavalent chromium ions.

EXPERIMENTAL WORK

Oil shale chemical activation

As a start, 50 grams of oil shale was activated using both 95% wt. H_2SO_4 and 5% wt. HNO_3 at 25 °C. The temperature of the product was increased rapidly to 150° indicating an exothermic reaction, as well as gas bubbling,was observed indicating that the reaction is taking place. Then, the solution was heated further to 270° on a hot plate while CO, SO_2, carbon monoxide, carbon, sulfur dioxide, and nitrous oxide(N_2O) were expelled out of the solution.

Once the product becomes solidified, it is cooled down to 25 °C, then washed with distilled water to remove any excess acids. The activated oil shale sample (AC) was further treated and mixed overnight with (1M) sodium hydroxide, and then heated in a closed vessel in an oven for 24 hrs. at 160°. The sample was washed to remove excess alkaline; afterwards, the sample was dried at 70° and stored. The obtained sample is assigned as (ACS).

ZVI stabilization on ACS

Initially, 1.5 gm of chitosan powder (100,000–300,000 g/mole) was dissolved in 80 ml (2%) acetic acid to ensure a homogenous solution, then 4.5 g of ZVI particles (less than 212 micrometers) was carefully incorporated into the mixture, and then 1.5 g of ACS material was added. The mixture was then stirred and added slowly to a 450 ml Sodium hydroxide, and then stored for twelve hours at room temperature. The mixture was then decanted to remove the solid product and then deionized water was used to eliminate Sodium Hydroxide. Finally, the obtained product was dried for 24 hours at 70 °C.

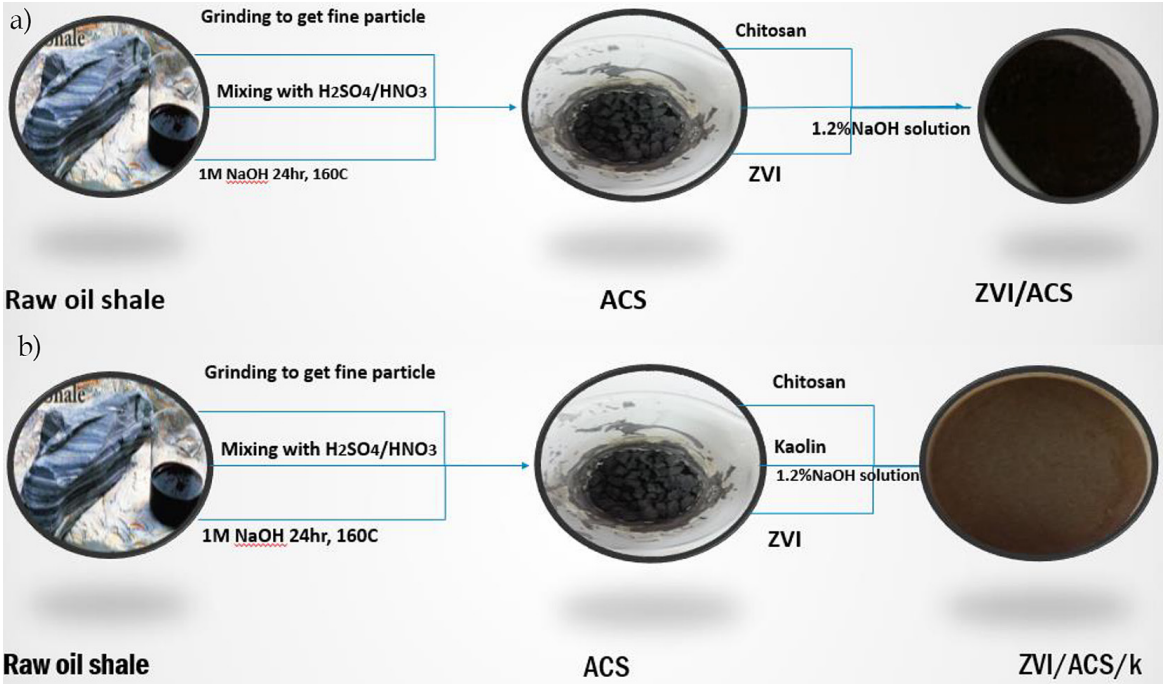

Figure 1. Experimental steps for the production of: A.(ZVI/ACS) B.(ZVI/ACS/K)

ZVI stabilization on ACS/Kaolin material

The same procedure in section 2.2 was repeated replacing the material ACS with (50 % wt. light kaolin: 50 % wt. ACS), and assigned as (ZVI/ACS) for ZVI supported on ACS material, and (ZVI/ACS/K) for ZVI supported on ACS and kaolin material. A schematic of the experimental steps of the production of the two materials is shown in Figure 1.

Adsorbents optimization

To evaluate the optimum condition of Cr (VI) adsorption by the produced composites, and have a better understanding of the adsorption characteristics, the effects of pH, and dosage, on the removal rate were investigated as discussed in the following sections.

Optimized pH

Adsorption experiments were carried out at different pH values: (10, 8, 6, and 3) at fixed adsorbent mass (0.05 g), which were added to 10 ml of 50 ppm potassium dichromate solution, for both ZVI/ACS and ZVI/ACS/K materials. The pH was controlled by adding drops of HCl or NaOH using a pH meter. After placing it in an

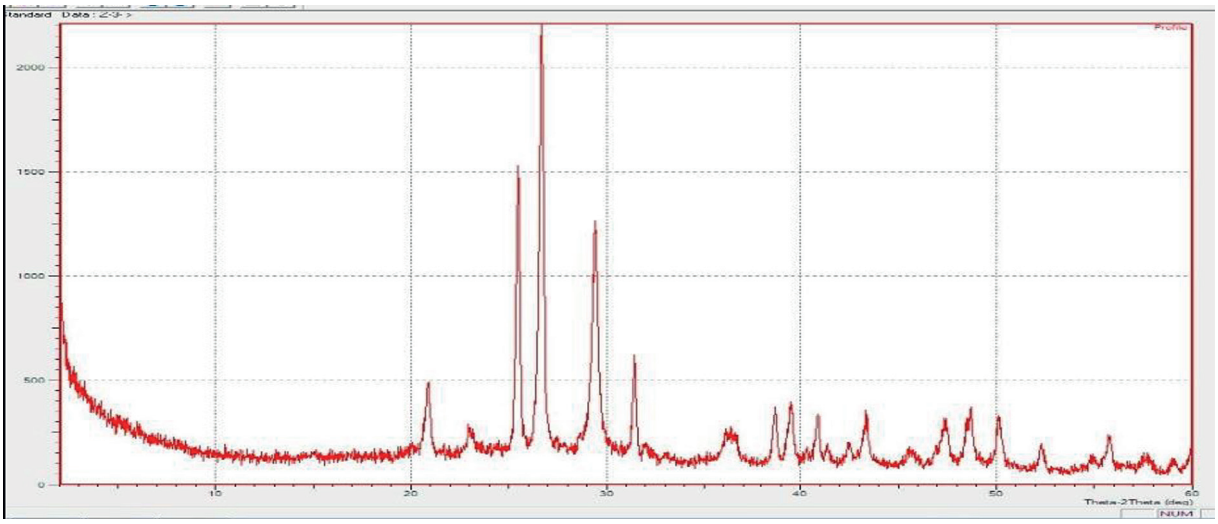

Figure 2. XRD analysis for ACS material before ZVI stabilization

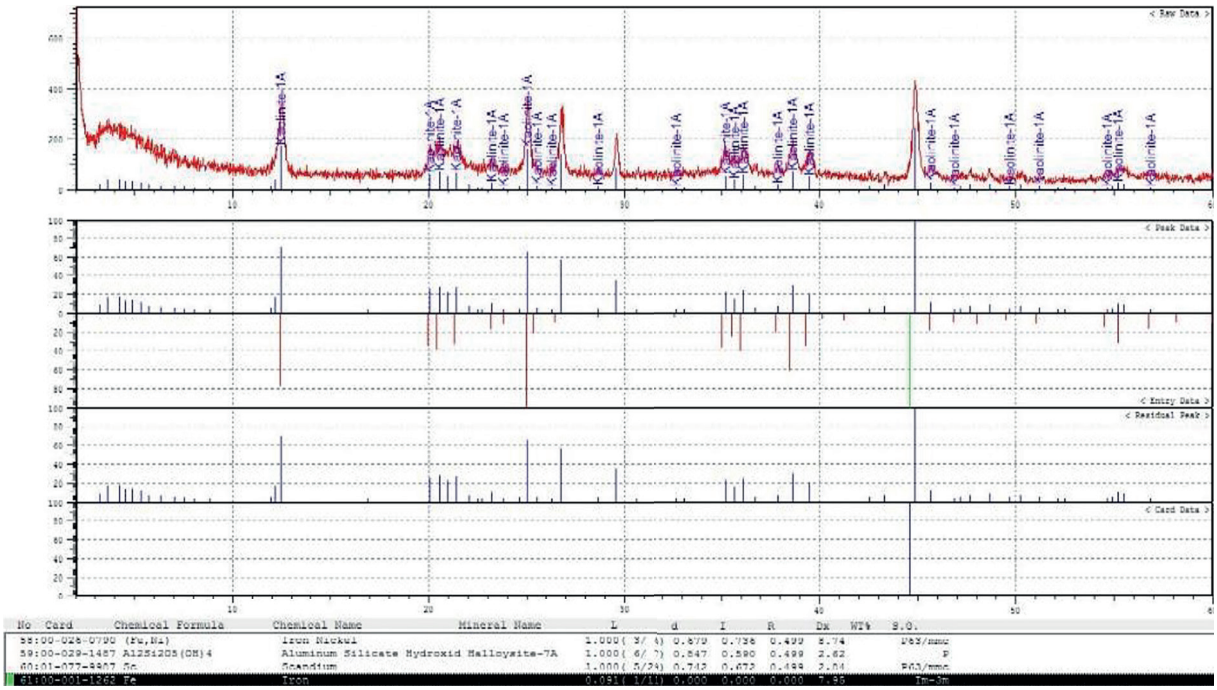

Figure 3. XRD analysis of ACS material after ZVI stabilization

isothermal shaker at (T = 27 °C) for 24 hrs, the solutions were filtered through a 0.45-micrometer filter paper; then, the residual Cr (VI) was estimated by a (UV) spectrophotometer.

Optimized dosage of the produced adsorbents

To optimize the dosage of the produced adsorbents, different amounts of each adsorbent were used at the optimized pH and a temperature of 27 °C. The amounts used were: 0.05, 0.1, 0.2, 0.4, and 0.5 g for both ZVI/ACS and ZVI/ACS/K adsorbents.

Another batch experiment was carried out at different initial concentrations of chromium (100 ppm, 200 ppm, 300 ppm) at pH 3 and fixed adsorbent mass of 0.2 g at two different temperatures (T = 27 °C, T = 50 °C).

RESULTS AND DISCUSSIONS

Characterization of adsorbents (ZVI/ACS, ZVI/ACS/K)

To determine the underlying crystal structure of the produced adsorbents and have a better understanding of the surface morphology, (XRD) analysis and (SEM) were carried out.

XRD analysis

XRD makes it possible to confirm the crystallinity and structure of a sample. Figure 2, represents the results of XRD conducted only on ACS before the stabilization process. The presence of ZVI on ACS, and ACS/K materials was confirmed by the XRD (Shimadzu -7000 maxima, Japan) analysis. The XRD patterns show that the ZVI/ACS and ZVI/ACS/K had additional diffraction peaks at 2 thetas of 45° corresponding to ZVI, as shown in Figures 3 and 4, respectively, which did not appear in Figure 2. The introduction of ZVI has changed the properties of the materials to be ferromagnetic that can be easily collected by a magnet.

SEM imaging

The images of (raw oil shale, AC, ACS, and ZVI/ACS/K) surfaces are obtained from a scanning electron microscope (SEM) model (Versa 3D, FEI). This analysis revealed the surface structure of the samples. SEM was carried out for the AC before and after treatment with NaOH to evaluate changes in their microstructures. In Figure 5a it may be noted that activation by acids has formed $CaSO_4$ (gypsum) and a variety of randomly distributed pore sizes due to the activation process. Comparing the two images, (5b and 5c) it can be inferred that a highly porous surface can be observed for the ACS due to the removal of $CaSO_4$ which resulted in a relatively more porous structure. In Figure 5d, the white color reveals the clay structure of the produced material and a randomly distributed pore size.

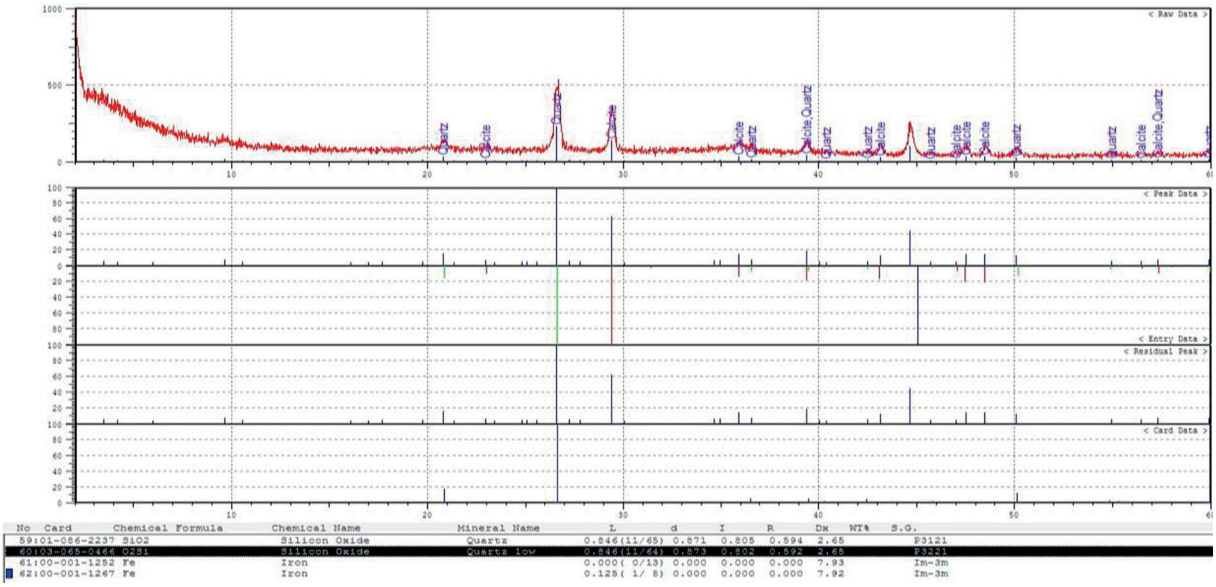

Figure 4. XRD analysis of ACS/K material after ZVI stabilization

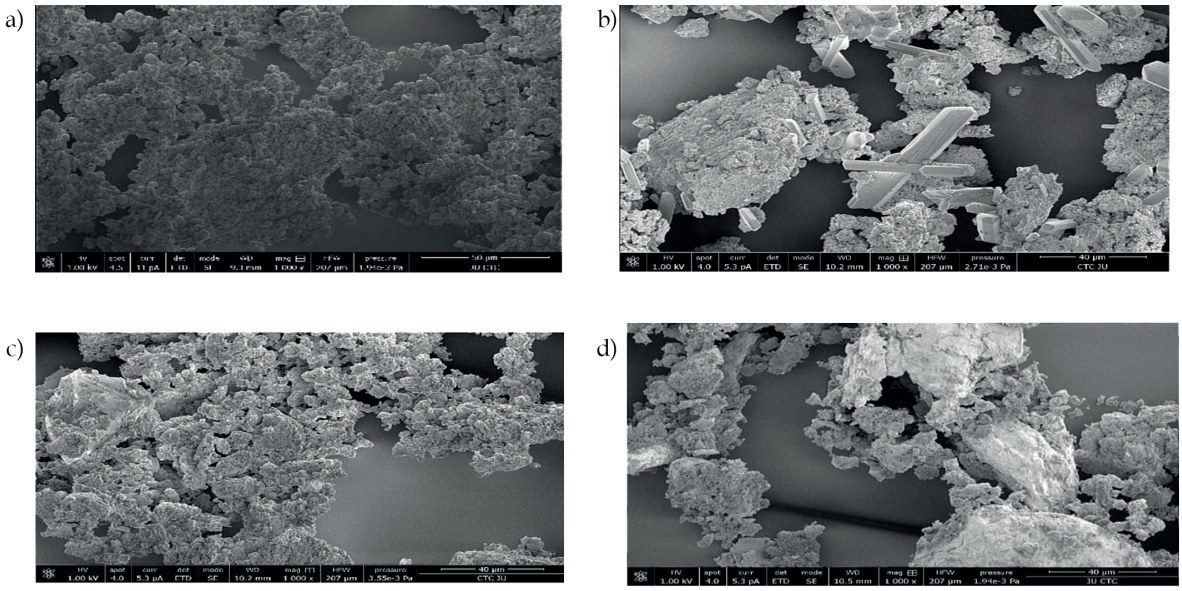

Figure 5. SEM images for: A. raw oil shale B. AC C. ACS D. ZVI/ACS/K

UV-visible spectrometry

Hexavalent chromium ion determination was performed using the direct method. As shown in Figure 6, the absorption band peaks at 348 nm. Another peak at 260 nm is noted, which is related to the charge transfer transition between the oxygen and the hexavalent chrome; however, this peak is not wide and maybe not be used for chromium presence (Hachair et al., 2018). At basic media (pH 10), there are two absorption bands. The first one peaks at 290 nm, which corresponds to the absorption of the chromium compound as a result of charge transfer between O_2 and Cr(VI). The maximum peak is at 375 nm. The change in the wavelength from 375 to 348 nm when changing from basic to acidic conditions can be explained by the formation of the hydrogen bond as well as the split of a bond between O_2 and the Cr ion. CrO_4^{-2} has higher absorbance, which means that it absorbs light at less energy than $HCrO_4$ or H_2CrO_4. (Hachiro et al., 2018).

Due to the impact of pH on Cr(VI) light absorption, two calibration curves were developed, one for basic circumstances (375 nm) at pH levels higher than 6.4 and one for acidic conditions (348 nm) at pH levels lower than Pka value (6.4). The calibration curve for acidic environments is shown in Figure 7. One can observe the linearity between 1 and 50 mg/L. Thus, the BeereLambert law can be used in this range. The linear equation is $y = 0.0268x + 0.0089$ with a correlation factor R^2 of 0.9988.

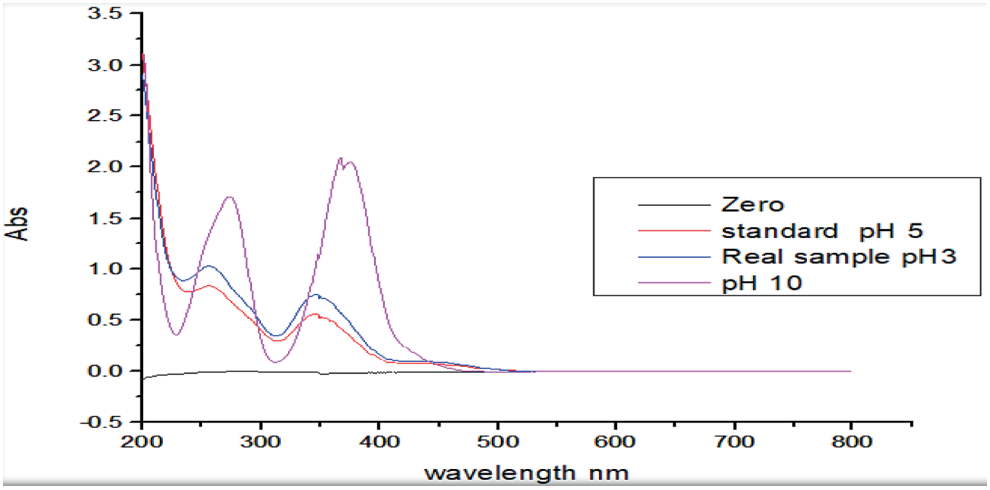

Figure 6. Spectral responses of a standard solution (red line), real sample (blue line) in acidic media, and areal sample in basic media (pink line)

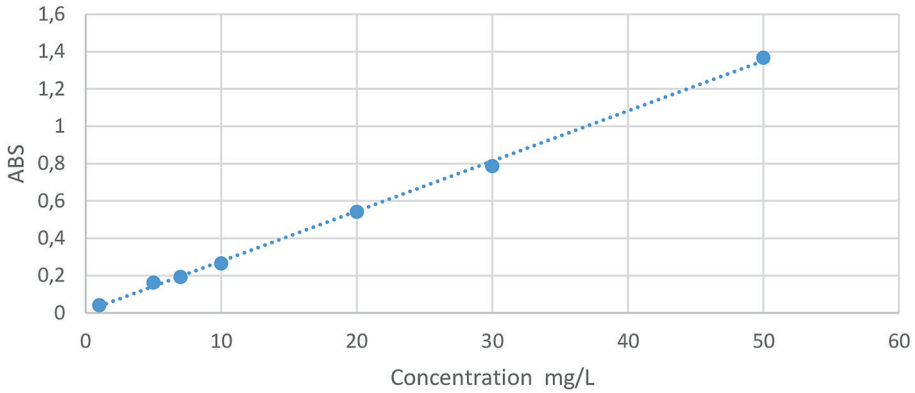

Figure 7. Calibration curve for the acidic condition at 348 nm

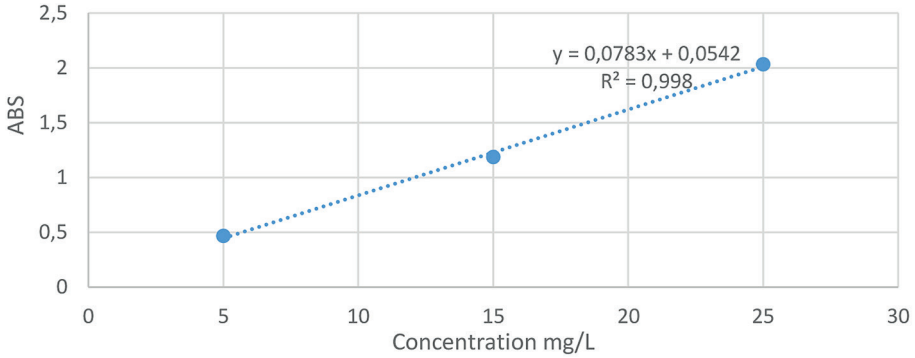

Figure 8. Calibration curve at 375 nm in basic conditions

Figure 8 shows the calibration curve for (pH 10), as indicated the relation is linear in the range between 5 and 25 mg/L, BeereLambert law can be applicable for this range of linearity, using the equation y = 0.078x + 0.0542 with a correlation factor R^2 of 0.998.

The removal rate of Cr (VI)

The absorption rate of chromium at certain pH values is shown in Figure 9; as indicated, Cr^{6+} was removed at low pH, while it decreases significantly at higher values both ZVI/ACS and ZVI/ACS/K. This is due to the pH effect on speciation of Cr(VI), in acidic media with pH values lower than Pka (6.5) the hexavalent chrome ion in the form of $HCrO_4^-$ dominates, while under basic conditions at pH higher than Pka (6.5) the main form of Cr in solution is CrO_4^{-2} *(*Lv et al., 2011*)*. $HCrO_4^-$ has less adsorption-free energy and more redox potential than CrO_4^{2}; therefore, it is favored in adsorption and easier to be reduced.

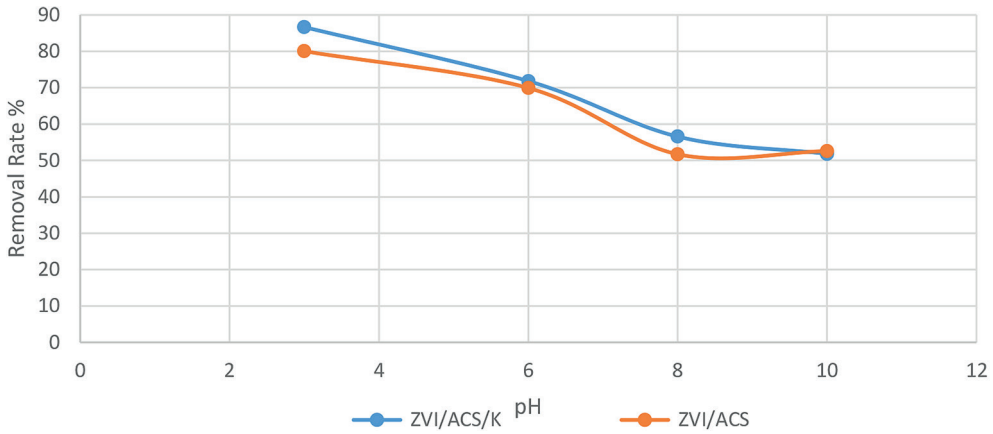

Figure 9. Removal rate of ZVI/ACS and ZVI/ACS/K at different pH values (3, 6,8,10, T = 27 °C, dose = 0.05g, time: 24hr)

The absorption of Cr(VI) by ZVI is highly affected by protons. The concentration of H^+ on the particle surface increases with the decrease of the pH, this leads to the strong electrostatic attraction between Cr(VI) and the particle (Shen et al., 2020a).

The UV spectra of Cr(VI) solutions are shown in Figure 10 both before and after the adsorption with ZVI/ACS/K material at an optimum pH value of 3. K_2CrO_4 solution indicates a UV-visible spectrum with absorption peaks at 273 nm and 370 nm (G Dong et al., 2011), while K2Cr2O7 solution gives out a spectrum with absorption peaks at 257 nm and 350 nm (red curve) After treatment with ZVI/ACS/K, $K_2Cr_2O_7$ solution shows an identical spectrum of K_2CrO_4 with absorption peaks at 273 nm and 370 nm (blue curve) which is consistent with the literature (G Dong et al., 2011). These results indicate that the $K_2Cr_2O_7$ is catalyzed by ZVI/ACS/K material, and transforms into K_2CrO_4 during the treatment.

Figure 11 shows the effect of ZVI/ACS and ZVI/ACS/K dosages on the reduction rate of Cr(VI). It may be noticed that it increases with the adsorbent dose up to an equilibrium dose value which is: (40 g/L, and 20 g/L) for ZVI/ACS, and ZVI/ACS/K respectively. The increase in removal rate with an adsorbent dose can be explained by a high adsorbent surface beside the availability of more adsorption active sites; at a higher dose than optimum, the removal rate of adsorbent was almost constant. The reason for this behavior is due to the possible overlapping or aggregation of adsorption sites, leading to a lower total surface area.

Figure 12, shows the removal rate of each adsorbent, it is noted that the introduction of ZVI on ACS & ACS/k materials has improved the removal rate from (73.9% to 90.9%) (73.9% to 98.5%), respectively, which confirmed the enhancement of the removal due to ZVI addition and chitosan coating, as chitosan has the amine

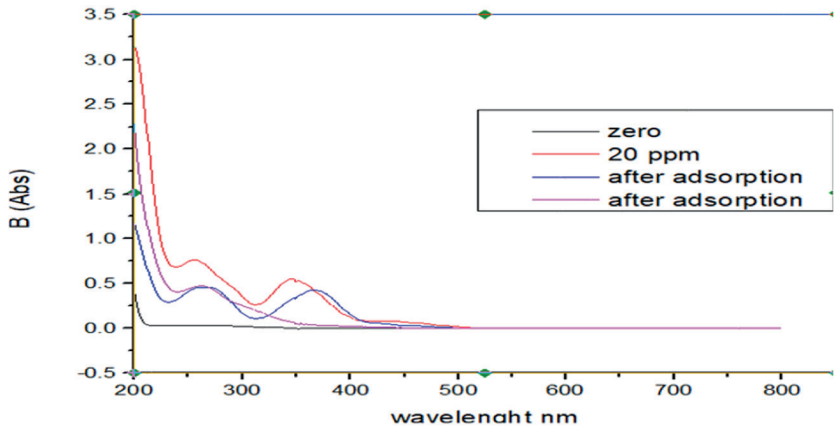

Figure 10. UV analysis after adsorption by ZVI/ACS/K, pH 3, 24 hr, initial concentration 50 ppm Cr(VI). Dosage 0.05 g

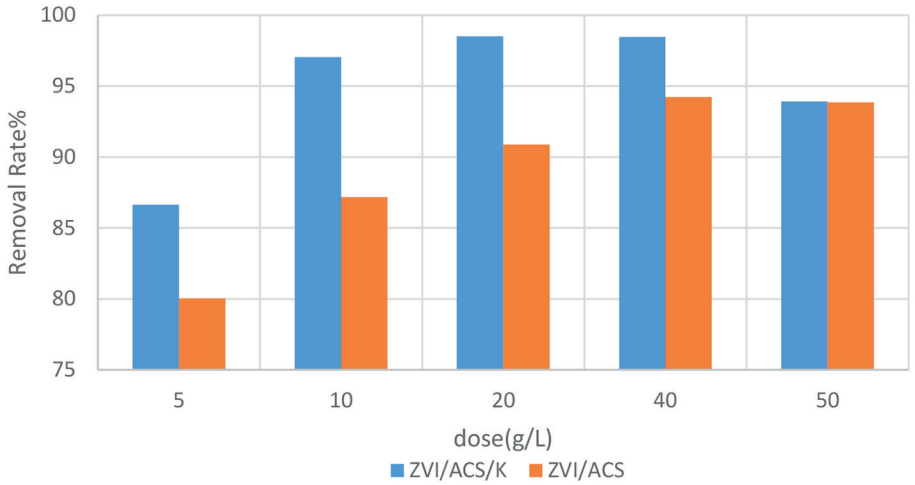

Figure 11. The effect of adsorbent dose of ZVI/ACS, ZVI/ACS/k on the removal rate (pH: 3, contact time: 24 hr., initial concentration 50 ppm Cr(VI), T = 27 °C)

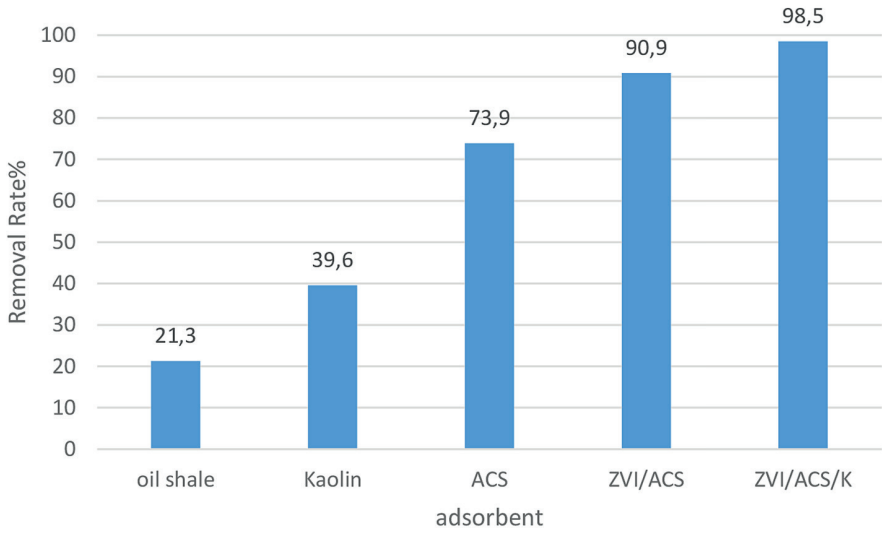

Figure 12. Removal rate of (raw oil shale, kaolin, ACS, ZVI/ACS / ZVI/ACS/K) at (pH: 3, time: 24 hr., dose: 20 g/L, T = 27 °C, initial concentrations 50 ppm Cr(VI))

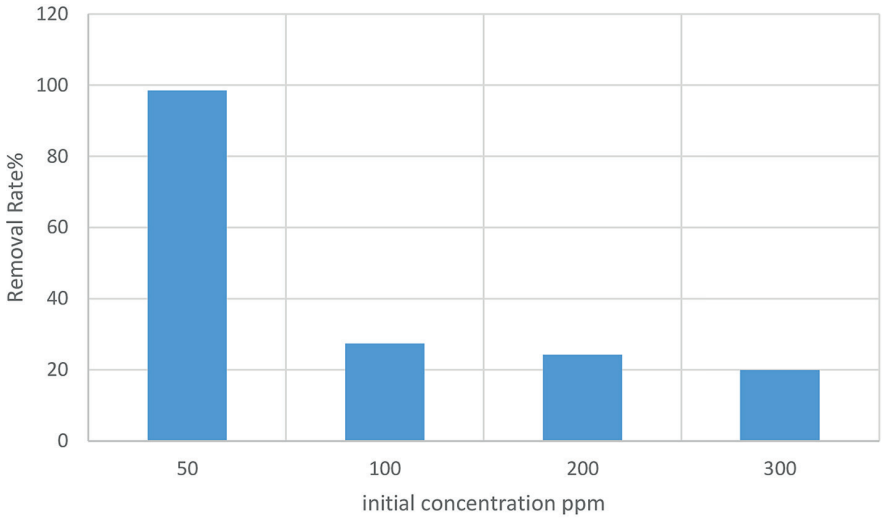

Figure 13. Removal Rate by ZVI/ACS/K at different initial concentrations (50 ppm, 100 ppm, 200 ppm, 300 ppm of Cr(VI)) (pH: 3, time: 24 hr., dose: 20 g/L, T = 27 °C)

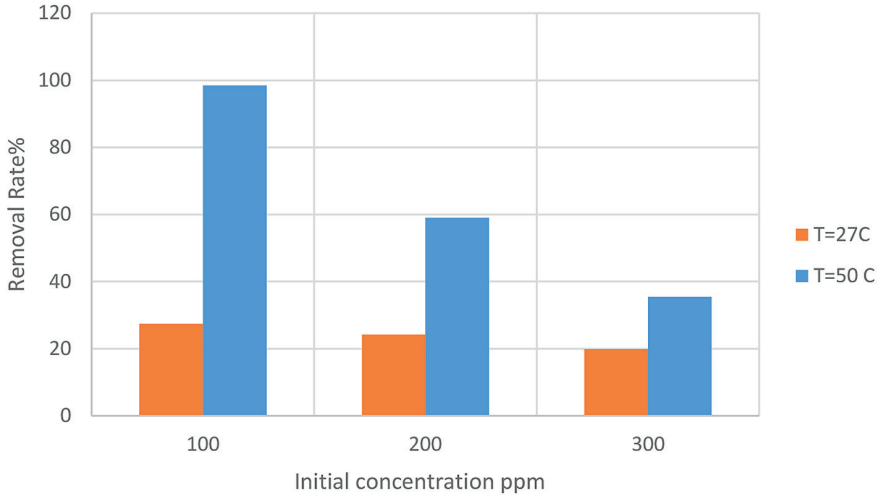

Figure 14. Removal Rate by ZVI/ACS/K at different initial concentrations (100 ppm, 200 ppm, 300 ppm of Cr(VI)) (pH: 3, time: 24 hr., dose: 20g/L, T = 50 °C)

groups that have significant chelation to cationic metal ions. On the other hand, the use of kaolin to stabilize ZVI has a remarkable effect in increasing the removal rate. These findings indicate that both the kaolin and the ZVI particles on the ACS surfaces played a major role in the increased removal of Cr(VI). This is in agreement with the findings of (Xi et al., 2010).

To study the dependency of the absorption rate of Cr on its initial concentration, a Cr of 50 to 300 ppm was used. As indicated in Figure 13, the removal rate of Cr by ZVI/ACS/K decreases with the initial concentration. This is because as initial chromium concentrations increase, the adsorbent surfaces will be saturated, which agrees with the results obtained by (Noraee et al., 2019).

Figure 14 illustrates that the increase in temperature from 27 to 50 °C results in enhanced reduction percentage from (27.4% to 98.5%), (24.2% to 59.0%), (19.5% to 35.5%) for the initial concentrations of 100 ppm, 200 ppm, and 300 ppm respectively. This is because of the dispersion of Cr(VI) ions and the higher kinetic energy of Cr(VI) ions heading toward the active sites of the adsorbent.

CONCLUSIONS

In this work, synthesis was developed to prepare ZVI/ACS and ZVI/ACS/K composite materials from Jordanian oil shale. The following points can be concluded. The presence of ZVI and light kaolin plays an important role in increasing the removal rate in the synthesized composite. The removal rate of hexavalent chrome by ZVI/ACS/K & ZVI/ACS is highly dependent on the pH value, with an optimum value at pH 3. The removal rate of hexavalent chrome by ZVI/ACS/K & ZVI/ACS was found to increase with the dosage until reaching the equilibrium dose. The ZVI/ACS/K has shown a better ability to remove hexavalent chrome ions from aqueous solutions than ZVI/ACS. The removal rate was found to decrease with increasing the initial hexavalent chrome concentrations. The optimized adsorption conditions of chromium ions by ZVI/ACS/K were: (pH: 3, T = 50 °C, dose: 0.2 g, initial concentration: 100 ppm). ZVI/ACS/K was found to be an effective adsorbent for the removal of crystal violet dye from aqueous solutions. The two produced composites are ferromagnetic and could be easily collected by a magnet.

REFERENCES

1. El Zayat, M. 2009. Removal of heavy metals by using activated carbon produced from cotton stalks. American University in Cairo, Thesis. AUC Knowledge Fountain. https://fount.aucegypt.edu/retro_etds/2289
2. Sounthararajah, D.P., Loganathan, P., Kandasamy, J., Vigneswaran, S. 2015. Effects of humic acid and suspended solids on the removal of heavy metals from water by adsorption onto granular activated carbon. International Journal of Environmental Research and Public Health, 12(9), 10475–10489.
3. Yahya, M.D., Kehinde, S.O., Abdulkadir M.B., Iyaka Y.A., Olugbenga, A.G. 2020. Characterization of cobalt ferrite-supported activated carbon for removal of chromium and lead ions from tannery wastewater via adsorption equilibrium. Water Science and Engineering 13(3), 202–213.
4. He, X., Min, X., Peng, T., Zhao, F., Ke, Y., Wang, Y.Wang, J. 2020. Mechanochemically activated microsized zero-valent iron/pyrite composite for effective hexavalent chromium sequestration in aqueous solution, Journal of Chemical & Engineering Data, 65(4).
5. Qu, G., Kou, L., Wang, T., Liang, D., Hu, S. 2017. Evaluation of activated carbon fiber supported nanoscale zero-valent iron for Chromium (VI) removal from groundwater in a permeable reactive column. Environ. Manage, 202, 387.
6. Zhou, Y., Gao, B., Zimmerman, R., Chen, H., Zhang, M., Cao, X. 2014. Biochar-supported zero-valent iron for removal of various contaminants from aqueous solutions. Bioresource Technology, 152, 538–542.
7. Congbin X., Chen Y., Xiaodan L., Yali H, Xing X, Yurong Z, Zhi Q, Jianzhong Z, Zhengping H. 2021. Agar-stabilized sulfidated microscale zero-valent iron: Its stability and performance in chromate reduction, Journal of Hazardous Materials, 417.
8. Lv X., et al. 2011. Removal of Chromium (VI) from wastewater by nanoscale zero-valent iron particles supported on multiwalled carbon nanotubes. Chemosphere, 85.7, 1204–1209.
9. Shen, W., Zhang, J., Xiao, M., Zhang, X., Li, J., Jiang, W., Yan, J., Qin, Z., Zhang, S., He, W., He, Y. 2020. Ethylenediaminetetra acetic acid induces surface erosion of zero-valent iron for enhanced hexavalent chromium removal. Applied Surface Science, 525, 146593.
10. Dong, G., Zhu, Y., Zhang, Y., Shan, H., Xu, J. 2011. study in Spectrophotometric study on kinetics and thermodynamics of adsorption and catalytic transformation of $K_2Cr_2O_7$ to K_2CrO_4 by natural hermit crab shell powder. Chemical Sciences Journal, 42.
11. Xi Y.F., Mallavarapu M., Naidu R. 2010. Reduction and adsorption of Pb_2^+ in aqueous solution by nano-zero-valent iron-a SEM, TEM and XPS study. Mater. Res. Bull., 45, 1361–1367.
12. Noraee, Z., Jafar, A., Ghaderpoori, M., Bahram, K., Ghaderpoury, A. 2019. Use of metal-organic framework to remove Chromium (VI) from aqueous solutions. Journal of Environmental Health Science and Engineering, 17, 701–709.